J. Fluid Mech. (1987), *vol.* 174, *pp.* 441–465
Printed in Great Britain

The gravitational settling of aerosol particles in homogeneous turbulence and random flow fields

By M. R. MAXEY
Division of Applied Mathematics, Brown University, Providence, RI 02912, USA

(Received 25 November 1985 and in revised form 6 June 1986)

The average settling velocity in homogeneous turbulence of a small rigid spherical particle, subject to a Stokes drag force, is shown to depend on the particle inertia and the free-fall terminal velocity in still fluid. With no inertia the particle settles on average at the same rate as in still fluid, assuming there is no mean flow. Particle inertia produces a bias in each trajectory towards regions of high strain rate or low vorticity, which affects the mean settling velocity. Results from a Gaussian random velocity field show that this produces an increased settling velocity.

1. Introduction

A primary question in the study of aerosol-particle motion is the effect of turbulence on the average settling velocity of the particles. This affects such things as the residence time of aerosol contaminants in the atmosphere and the growth rate of water droplets falling under gravity. In still fluid, away from confining walls, it is relatively straightforward to determine the terminal fall speed under gravity. Extensive measurements have been made for particles of both spherical and non-spherical shape over a wide range of sizes, and these results are well summarized for example by Clift, Grace & Weber (1978). In a turbulent flow an aerosol particle is subject to fluctuating drag forces produced by the turbulent velocity fluctuations in the surrounding fluid. Its motion is also determined by the effects of gravitational settling and inertia of the particle, while such effects as Brownian motion are not significant if the particle is large enough. It is not clear what the effect of these fluctuating forces will be on the ensemble-averaged settling velocity, and whether or not in the absence of a mean flow in homogeneous turbulence the particles will settle asymptotically at the same rate as they would in still fluid.

Most attention in the past has focused on the dispersion of particles by turbulence, and the question of settling velocities has largely been ignored. Theoretical work in this area has been done by Tchen (1947), Yudine (1959), Csanady (1963), Meek & Jones (1973), Reeks (1977, 1980) and Nir & Pismen (1979). It was Yudine (1959) who noted the 'crossing-trajectories effect' for particles settling under gravity, whereby particles move relative to the surrounding fluid and cross the Lagrangian trajectories of fluid elements. The net result is for the velocity autocorrelation of the particles to decay more rapidly than for fluid elements and for the dispersion to be reduced. Csanady (1963) further showed that, for rapidly settling particles, the turbulent-dispersion coefficient in the vertical direction may be up to twice that in the horizontal direction owing to the 'continuity effect' in incompressible turbulent flow. The papers by Tchen, Meek & Jones, Reeks and Nir & Pismen have studied the influence of particle inertia on the turbulent-dispersion process based on various models or closure assumptions. Experiments by Snyder & Lumley (1971), and by

Wells & Stock (1983) have generally confirmed the conclusions of these studies, as have the numerical simulations of Riley (1971), Riley & Patterson (1974), and Reeks (1980). These experiments and simulations were primarily for particles either with settling velocities large compared with the level of the turbulent-velocity fluctuations or zero settling velocity. No change in the settling velocities due to the turbulence was reported in these.

Reeks (1977) has argued that in homogeneous turbulence there would be no net effect on the average settling velocity. Indeed, in the absence of particle inertia it may be established, as shown in the next section, that for homogeneous, stationary turbulence the average particle velocity is just the sum of the terminal fall velocity in still fluid and the Eulerian mean flow velocity. On the other hand, a recent study by Maxey & Corrsin (1986) has shown that owing to the influence of particle inertia, particles in a random cellular flow field may settle out significantly more rapidly than in still fluid. In this study the flow field was two-dimensional, incompressible and periodic in both x_1, x_2 coordinates with a stream function ψ

$$\psi(x_1, x_2) = U_0 L \sin\left(\frac{x_1}{L}\right) \sin\left(\frac{x_2}{L}\right).$$

In each realization of the experiment a spherical Stokes particle was introduced at some random location and the direction of the gravitational acceleration $\boldsymbol{g}$ was selected at random in the (x_1, x_2)-plane. The subsequent particle motion was computed by numerically integrating the equations of particle motion, and the components of particle velocity parallel and perpendicular to $\boldsymbol{g}$ were recorded. Averages were then made over a large number of realizations of the experiment. If $W^{(s)}$ denotes the Stokes settling velocity in still fluid, the increase in settling rates was most pronounced for $W^{(s)}/U_0 \leqslant 1$ but was negligible for $W^{(s)}/U_0 > 2$. Particle inertia also had the surprising effect of causing particles, for a given direction and value of $\boldsymbol{g}$, to accumulate along isolated and well-defined curves.

The aim of this paper is to investigate whether in general particle settling velocities in homogeneous, stationary turbulence differ from those in still fluid, and in particular to investigate the role played by particle inertia. In the following section the problem is formulated more precisely, then in §3 results are given from numerical simulations of particle motion in a Gaussian, random velocity flow field. These results are then considered in terms of various asymptotic limits of either rapid settling or weak particle inertia.

2. Aerosol-particle motion

2.1. *Equation of particle motion*

The equation of motion for a small spherical aerosol particle of radius a and mass m_p is

$$m_p \frac{\mathrm{d}\boldsymbol{V}}{\mathrm{d}t} = 6\pi a\mu(\boldsymbol{u}(\boldsymbol{Y}(t), t) - \boldsymbol{V}(t)) + m_p \boldsymbol{g}, \tag{2.1}$$

where $\boldsymbol{Y}(t)$, $\boldsymbol{V}(t)$ are the position and velocity of the particle, $\boldsymbol{g}$ is the acceleration due to gravity and μ is the dynamic viscosity of the surrounding fluid. The flow field $\boldsymbol{u}(\boldsymbol{x}, t)$ of the surrounding fluid is incompressible. The equation represents a balance of particle inertia and acceleration, with the fluid drag force produced by the motion of the particle relative to the surrounding fluid and the force due to gravity. A Stokes drag law has been assumed in (2.1) and this is appropriate if the particle size is sufficiently small that the Reynolds number for the relative motion of the particle through the fluid is significantly less than one. The particle is also assumed to be much smaller than the lengthscales associated with the flow field $\boldsymbol{u}(\boldsymbol{x},t)$. In a turbulent flow this leads to the condition that $a \ll \eta_K$, where η_K is the Kolmogorov microscale, Maxey & Riley (1983). For an aerosol particle, such as a water droplet in air, the density of the particle is much greater than that of the surrounding fluid so that buoyancy forces, added-mass and other effects are negligible while the particle-inertia term may still be significant. The particle is further supposed to be sufficiently large that Brownian motion is negligible. Particle concentrations or number density will be assumed to be very low, so that the particles move independently of each other and do not modify the flow field. Despite the restrictions that have been imposed, (2.1) is applicable to many different aerosol problems: in air flows under most atmospheric conditions (2.1) would apply for example to aerosol particles in the range 2 μm $< a <$ 30 μm (Pruppacher & Klett 1978).

The equation of motion (2.1) may be divided by the particle mass and written in the form

$$\frac{\mathrm{d}\boldsymbol{V}}{\mathrm{d}t} = \alpha(\boldsymbol{u}(\boldsymbol{Y}(t),t) - \boldsymbol{V}(t) + \boldsymbol{W}^{(\mathrm{s})}), \tag{2.2}$$

where we have introduced the Stokes settling velocity $\boldsymbol{W}^{(\mathrm{s})}$, the terminal fall velocity in still fluid,

$$\boldsymbol{W}^{(\mathrm{s})} = \frac{m_{\mathrm{p}}\boldsymbol{g}}{6\pi a\mu}, \tag{2.3}$$

and α, the response 'frequency' of the particle to changes in the flow conditions surrounding the particle,

$$\alpha = \frac{6\pi a\mu}{m_{\mathrm{p}}}. \tag{2.4}$$

The problem of interest is to determine the ensemble-averaged velocity $\langle \boldsymbol{V}(t)\rangle$ of a particle in a turbulent flow. In statistically homogeneous and stationary turbulence this average will reach some asymptotic stationary value, long after the particle release. From an average of (2.2) this asymptotic value must satisfy, as $t \rightarrow \infty$,

$$\langle \boldsymbol{V}(t)\rangle = \boldsymbol{W}^{(\mathrm{s})} + \langle \boldsymbol{u}(\boldsymbol{Y}(t),t)\rangle. \tag{2.5}$$

The average $\langle \boldsymbol{u}(\boldsymbol{Y}(t),t)\rangle$ is the ensemble-averaged fluid velocity as measured following a particle trajectory. Both the velocity field $\boldsymbol{u}$ and the particle position $\boldsymbol{Y}$ exhibit statistical fluctuations, and this average differs in nature from both a Eulerian, fixed-point average and a Lagrangian average following a fluid element. Whether or not the turbulence has a net effect on settling rates depends on whether or not this average is equal to the Eulerian mean fluid velocity $\boldsymbol{U}^{(0)}$.

2.2. *Settling in the absence of particle inertia*

If particle inertia is completely neglected (2.2) simply reduces to the statement that the particle velocity is the sum of the still-fluid settling velocity and the instantaneous velocity of the surrounding fluid. This may be written as

$$\frac{\mathrm{d}\boldsymbol{Y}}{\mathrm{d}t} \equiv \boldsymbol{V}(t) = \boldsymbol{v}(\boldsymbol{Y}(t),t), \tag{2.6}$$

$$\boldsymbol{v}(\boldsymbol{x},t) = \boldsymbol{u}(\boldsymbol{x},t) + \boldsymbol{W}^{(\mathrm{s})}, \tag{2.7}$$

where we have introduced $\boldsymbol{v}(\boldsymbol{x},t)$ as a 'flow field' for the particles. As $\boldsymbol{W}^{(\mathrm{s})}$ is simply a constant and the fluid flow field is incompressible it follows that $\boldsymbol{v}(\boldsymbol{x},t)$ is also incompressible. The equation for particle motion (2.6) however now has the same form as a Lagrangian material element moving in the 'flow field' $\boldsymbol{v}(\boldsymbol{x}, t)$. Lumley (1962) (see also Tennekes & Lumley 1972) has shown that for homogeneous and stationary turbulence in an incompressible flow the one-point Eulerian statistics and the one-point Lagrangian statistics of the flow field are equal. The immediate conclusion is then that $\langle \boldsymbol{V}(t) \rangle$ equals the Eulerian mean value of $\boldsymbol{v}$, namely

$$\langle \boldsymbol{V}(t) \rangle = \boldsymbol{U}^{(0)} + \boldsymbol{W}^{(\mathrm{S})}. \tag{2.8}$$

Thus if there is no inertia the turbulence itself has no net effect on the settling rate, and any effect necessarily requires the influence of particle inertia.

The same conclusion may also be drawn if the Stokes drag law (2.1) is replaced by a more general, nonlinear drag law dependent on the instantaneous Reynolds number of the relative motion. In terms of a dimensionless drag coefficient C_D, dependent only on the Reynolds number R, the equation of particle motion for negligible inertia is

$$0 = -\tfrac{1}{2} C_D(R)\, \pi a^2 \rho |\boldsymbol{w}(t)| \boldsymbol{w}(t) + m_{\mathrm{p}} \boldsymbol{g}, \tag{2.9a}$$

$$\boldsymbol{w}(t) \equiv \boldsymbol{V}(t) - \boldsymbol{u}(\boldsymbol{Y}(t), t), \tag{2.9b}$$

$$R = \frac{2a\rho |\boldsymbol{w}(t)|}{\mu}, \tag{2.9c}$$

where ρ is the density of the surrounding fluid. The modulus of (2.9a) gives then

$$C_D(R) \times R^2 = \frac{8 m_{\mathrm{p}} g \rho}{\pi \mu^2}, \text{ constant}; \tag{2.10}$$

implying that the Reynold number R and the drag coefficient C_D are constant. As with the linear Stokes drag law the particle velocity at any instant is the sum of the local, instantaneous fluid velocity $\boldsymbol{u}(\boldsymbol{Y}(t), t)$ and the constant, terminal fall velocity for still fluid

$$\boldsymbol{w}(t) = \boldsymbol{W}^{(\mathrm{T})} \equiv \frac{4 m_{\mathrm{p}} \boldsymbol{g}}{\pi \mu a C_D R}, \tag{2.11a}$$

$$R = \frac{2a\rho W^{(\mathrm{T})}}{\mu}. \tag{2.11b}$$

The motion of each particle is determined as before by (2.6) and (2.7), with $\boldsymbol{W}^{(\mathrm{T})}$ replacing $\boldsymbol{W}^{(\mathrm{S})}$, and the argument follows as before. Throughout the rest of this paper the Stokes drag law as in (2.1) will be assumed, but for more general drag-law relationships qualitatively similar results may be expected to apply.

2.3. *Scalings for isotropic, homogeneous turbulence*

The conditions under which particle inertia is important depend on the scales of the turbulent flow field compared to the inertial response frequency α. Attention will be restricted to statistically stationary, homogeneous and isotropic turbulence with zero mean flow, $\boldsymbol{U}^{(0)} = 0$. The fluctuations in fluid velocity will be scaled by u' defined in terms of the mean-square velocity fluctuation

$$u'^2 = \langle u_1^2(\boldsymbol{x}, t) \rangle. \tag{2.12}$$

The lengthscale L is defined in terms of the energy-spectrum function $E(k)$ for isotropic turbulence, defined in the usual manner (Batchelor 1953) so that

$$\tfrac{3}{2}\langle u_1^2(\boldsymbol{x}, t) \rangle = \int_0^\infty E(k)\, \mathrm{d}k. \tag{2.13}$$

The length L is chosen to be $1/k_*$, where k_* is the wavenumber at which $E(k)$ has a maximum. The scale L is thus characteristic of the larger, energetic eddies.

We also introduce for future reference the Eulerian, two-point, space–time correlation for homogeneous, stationary turbulence

$$R_{ij}(\boldsymbol{r};\tau) = \langle u_i(\boldsymbol{x},t)\, u_j(\boldsymbol{x}+\boldsymbol{r},t+\tau)\rangle, \tag{2.14}$$

which for isotropic turbulence has the general form

$$R_{ij}(\boldsymbol{r};\tau) = g(r,\tau)\,\delta_{ij} + [f(r,\tau)-g(r,\tau)]\frac{r_i r_j}{r^2}, \tag{2.15}$$

where $r = |\boldsymbol{r}|$. The condition of incompressible flow implies that

$$0 = \frac{\partial}{\partial r}f(r,\tau) + \frac{2}{r[f(r,\tau)-g(r,\tau)]}. \tag{2.16}$$

The generalized spectrum tensor $\Phi_{ij}(\boldsymbol{k};\omega)$ is defined as the Fourier transform of $R_{ij}(\boldsymbol{r},\tau)$ and is

$$\Phi_{ij}(\boldsymbol{k};\omega) = (2\pi)^{-4}\iiint_{-\infty}^{\infty} \mathrm{d}^3\boldsymbol{r}\, \mathrm{e}^{-\mathrm{i}\boldsymbol{k}\cdot\boldsymbol{r}} \int_{-\infty}^{\infty} \mathrm{d}\tau\, \mathrm{e}^{-\mathrm{i}\omega\tau} R_{ij}(\boldsymbol{r};\tau) \tag{2.17}$$

which for isotropic turbulence has the form

$$\Phi_{ij}(\boldsymbol{k};\omega) = \phi(k,\omega)\left[\delta_{ij} - \frac{k_i k_j}{k^2}\right], \tag{2.18}$$

where $k = |\boldsymbol{k}|$. The condition of compressible flow is satisfied by (2.18), requiring simply that

$$\Phi_{ij}k_j = k_i\Phi_{ij} = 0. \tag{2.19}$$

The standard spectrum tensor $\Psi_{ij}(\boldsymbol{k})$ is defined as the spatial Fourier transform of $R_{ij}(\boldsymbol{r};\tau=0)$, which may have derived from a knowledge of Φ_{ij},

$$\Psi_{ij}(\boldsymbol{k}) = \int_{-\infty}^{\infty} \Phi_{ij}(\boldsymbol{k};\omega)\,\mathrm{d}\omega.$$

From Ψ_{ij} the standard expression for the energy-spectrum function is

$$E(k) = \frac{1}{2}\iint_{|\boldsymbol{k}|=k} \Psi_{ii}(\boldsymbol{k})\,\mathrm{d}S(k),$$

where the integration is over spherical surfaces of radius k in wavenumber space. In terms of the function $\phi(k,\omega)$

$$E(k) = 4\pi k^2 \int_{-\infty}^{\infty} \phi(k,\omega)\,\mathrm{d}\omega. \tag{2.20}$$

The equation of particle motion may be scaled in terms of u' and L, and the following dimensionless variables introduced:

$$t^* = \frac{u't}{L},\quad \boldsymbol{x}^* = \frac{\boldsymbol{x}}{L},\quad \boldsymbol{Y}^* = \frac{\boldsymbol{Y}}{L},\quad \boldsymbol{V}^* = \frac{\boldsymbol{V}}{u'},\quad \boldsymbol{u}^* = \frac{\boldsymbol{u}}{u'}.$$

The resulting equation of motion is

$$\frac{1}{A}\frac{\mathrm{d}\boldsymbol{V}^*}{\mathrm{d}t^*} = \boldsymbol{u}^*(\boldsymbol{Y}^*(t^*),t^*) - \boldsymbol{V}^*(t^*) + \boldsymbol{W}. \tag{2.21}$$

The governing dimensionless parameters are the dimensionless settling velocity for still fluid

$$\boldsymbol{W} = \frac{\boldsymbol{W}^{(\mathrm{s})}}{u'}, \tag{2.22}$$

and the dimensionless inertia parameter

$$A = \frac{\alpha L}{u'} = \frac{\alpha}{k_* u'}. \tag{2.23}$$

The importance of particle inertia in a given situation is determined by the value of A. When A is large the inertia term is small and the particle responds rapidly to changes in the surrounding flow field. While if the value of A is small the particle inertia has a strong influence on the particle motion.

The scaled equation of motion (2.21) will be used henceforth and the asterisks will be suppressed. The motion of an individual particle is found by solving

$$\frac{1}{A}\frac{\mathrm{d}\boldsymbol{V}}{\mathrm{d}t} = \boldsymbol{u}(\boldsymbol{Y}(t), t) - \boldsymbol{V}(t) + \boldsymbol{W}, \tag{2.24}$$

subject to initial conditions for $\boldsymbol{Y}(t=0)$ and $\boldsymbol{V}(t=0)$.

3. Numerical simulations in a Gaussian random flow field

Following the methods used by Kraichnan (1970), Riley (1971) and Reeks (1980), we have computed the motion of aerosol particles in an incompressible, random flow field generated as a series of randomly selected Fourier modes. This technique is simpler than direct numerical simulations of turbulence (Riley & Patterson 1974), yet provides useful information. The joint velocity statistics of the resulting flow field are Gaussian, thus once the two-point correlations are specified all other statistical information may be derived. By suitable mode selection procedures it is possible to generate a statistically stationary, homogeneous and isotropic random flow with a prescribed two-point correlation $R_{ij}(\boldsymbol{r}, \tau)$. Unlike a genuine turbulent flow the triple correlations vanish and there is no representation of the energy transfer from large scales to smaller dissipative scales or of the advection of small-scale turbulent motions by the larger eddies. This is not serious if the range of lengthscales that are energetic is limited, as for the energy spectrum used here.

3.1. *Simulation method*

For each run of the simulation a flow field is generated as a sum

$$u_i(\boldsymbol{x}, t) = \sum_{n=1}^{N} \{b_i^{(n)} \cos(\boldsymbol{k}^{(n)}\cdot\boldsymbol{x} + \omega^{(n)} t) + c_i^{(n)} \sin(\boldsymbol{k}^{(n)}\cdot\boldsymbol{x} + \omega^{(n)} t)\}, \tag{3.1}$$

where N modes, typically 64, are selected independently and at random. First for each n, $\boldsymbol{k}^{(n)}$ and $\omega^{(n)}$ are chosen independently with probability-density functions

$$p_1(\boldsymbol{k}) = (2\pi k_0^2)^{-\frac{3}{2}} \exp\left(-\frac{k^2}{2k_0^2}\right), \tag{3.2a}$$

$$p_2(\omega) = (2\pi \omega_0^2)^{-\frac{1}{2}} \exp\left(-\frac{\omega^2}{2\omega_0^2}\right). \tag{3.2b}$$

Secondly real coefficients $\hat{b}_i^{(n)}$ and $\hat{c}_i^{(n)}$ are selected independently and at random according to a Gaussian probability function with zero mean and unit covariance matrix, so that on average

$$\langle \hat{b}_i^{(n)} \hat{b}_j^{(n)} \rangle = \delta_{ij}, \tag{3.3}$$

with a similar result for $\hat{c}_i^{(n)}$. Finally the coefficients are filtered and scaled according to the rule

$$b_i^{(n)} = \Gamma(k = |\boldsymbol{k}^{(n)}|, \omega = \omega^{(n)}) \left[\delta_{ij} - \frac{k_i^{(n)} k_j^{(n)}}{k^{(n)2}} \right] \hat{b}_j^{(n)}, \qquad (3.4)$$

to obtain the final coefficients. The filtering procedure ensures that $\boldsymbol{b}^{(n)} \cdot \boldsymbol{k}^{(n)}$ and $\boldsymbol{c}^{(n)} \cdot \boldsymbol{k}^{(n)}$ vanish, so that overall the flow field is incompressible. Furthermore, by averaging over a large number of different runs we generate a flow field that statistically is stationary, homogeneous and isotropic. The velocity statistics are Gaussian provided N is large enough.

A suitable choice of the scaling function $\Gamma(k, \omega)$ allows a random flow field to be generated with any prescribed two-point correlation. Since each mode is generated identically yet independent of the others, the averaged two-point correlation is

$$R_{ij}(\boldsymbol{r}; \tau) = N \iiint_{-\infty}^{\infty} \mathrm{d}^3\boldsymbol{k} \int_{-\infty}^{\infty} \mathrm{d}\omega \left\{ p_1(\boldsymbol{k})\, p_2(\omega)\, \Gamma^2(k, \omega) \left[\delta_{ij} - \frac{k_i k_j}{k^2} \right] \cos\,(\boldsymbol{k} \cdot \boldsymbol{r} + \omega\tau) \right\}, \qquad (3.5)$$

obtained by evaluation of (2.14) from the series (3.1) and the properties of the coefficients. A comparison with (2.17), (2.18) for $\Phi_{ij}(\boldsymbol{k}; \omega)$ shows that

$$\phi(k, \omega) = N p_1(\boldsymbol{k})\, p_2(\omega)\, \Gamma^2(k, \omega). \qquad (3.6)$$

For the simulations reported here the scaling function Γ was chosen to be

$$\Gamma(k, \omega) = \frac{(2N)^{-\frac{1}{2}} k}{k_0}, \qquad (3.7)$$

corresponding to a choice of the energy-spectrum function

$$E(k) = (2\pi)^{-\frac{1}{2}} \frac{k^4}{k_0^5} \exp\left(-\frac{k^2}{2k_0^2} \right). \qquad (3.8)$$

This choice of energy spectrum has also been used by Kraichnan (1970) and Reeks (1980). The function $E(k)$ in (3.8) has a maximum at $k = 2k_0$, so in view of the non-dimensional scalings in terms of k_* the value $k_0 = \frac{1}{2}$ is assigned. For this selection of $\Gamma(k, \omega)$ some standard correlations are

$$R_{11}(r, 0, 0; \tau = 0) \equiv f(r, \tau = 0) = \exp\,(-\tfrac{1}{2} k_0^2 r^2) \qquad (3.9)$$

for the longitudinal spatial correlation, and

$$R_{11}(\boldsymbol{r} = 0; \tau) = \exp\,(-\tfrac{1}{2} \omega_0 \tau^2), \qquad (3.10)$$

for the Eulerian time correlation. The corresponding integral lengthscale for (3.9) L_f and the corresponding Eulerian integral time scale T_E are

$$L_f = (2\pi)^{\frac{1}{2}}, \quad T_E = \frac{(2\pi)^{\frac{1}{2}}}{2\omega_0}. \qquad (3.11)$$

For each run of the simulation a random flow field (3.1) is generated as described above and a particle is released at the origin at $t = 0$ with the initial conditions

$$\boldsymbol{Y}(t = 0) = 0, \quad \boldsymbol{V}(t = 0) = \boldsymbol{W}. \qquad (3.12)$$

The particle motion is found by numerically solving (2.24), evaluating $\boldsymbol{u}(\boldsymbol{Y}(t), t)$ from (3.1) as required. This procedure is repeated so that each sample contains 1000 particles and averages for the velocity statistics are obtained by summing over all the particles. The computations were made to at least $t = 15$ and the asymptotic,

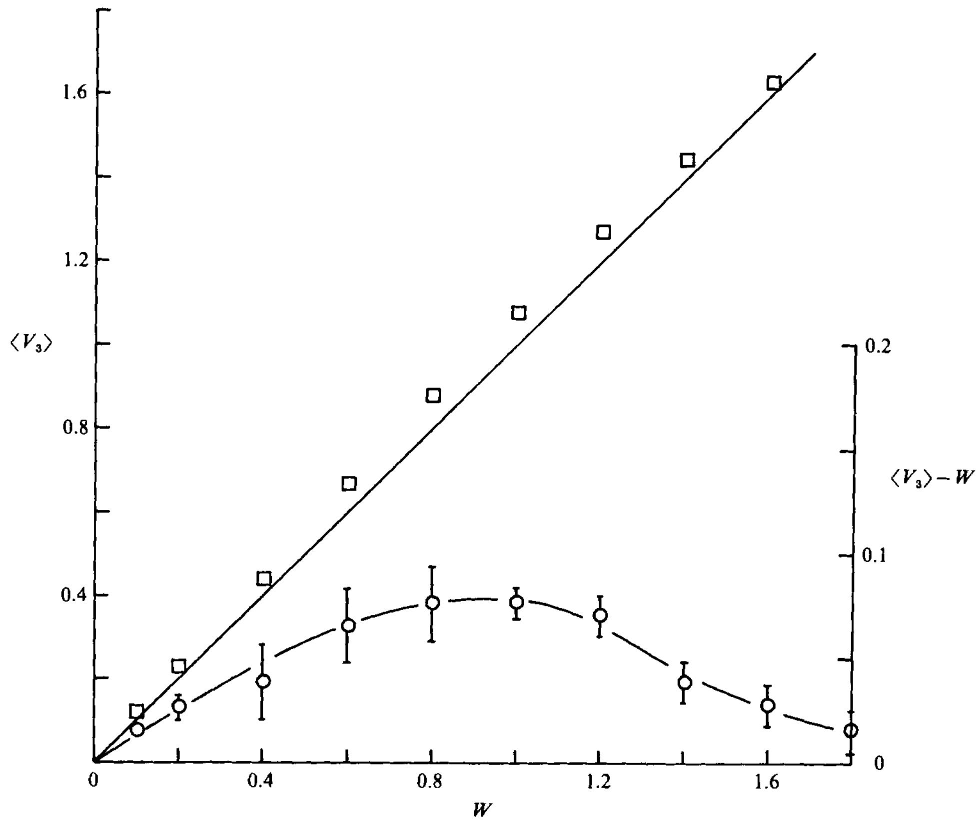

FIGURE 1. Simulation results for asymptotic average settling velocity $\langle V_3 \rangle$ against still-fluid settling velocity W; inertia parameter $A = 1$ and $\omega_0 = 0$: □, $\langle V_3 \rangle$; ○, increase in settling velocity $\langle V_3 \rangle - W$. Error bars show possible statistical error within one standard error of the mean.

steady-state statistics were estimated by further time-averaging the values between $t = 6$ and 15. Tests were made to ensure accuracy and convergence of the results, as well as to verify the Gaussian statistical properties of the flow field. In various instances, experiments were repeated several times to further reduce statistical errors. The differential equations were solved using the ISML subroutine DGEAR as a variable-order, variable-step-size, Adams predictor–corrector method (Rice 1983). The computations were carried out in double precision on the Brown University IBM 3081 computer.

3.2. *Simulation results*

Figure 1 shows the variations in the asymptotic average settling velocity $\langle V_3 \rangle$ for different values of the still-fluid settling velocity W, with the inertia parameter $A = 1$. The flow field is static in time, with $\omega_0 = 0$ and an infinite Eulerian integral timescale T_E. In all the simulations the still-fluid settling velocity W was taken to be in the x_3 direction. Since the flow field is statistically isotropic, this is the only preferred direction in determining the average velocity statistics, and the results thus depend only on whether the velocity component is parallel or perpendicular to $\boldsymbol{W}$. Indeed $\langle V_1 \rangle$ and $\langle V_2 \rangle$ were found to be zero to within statistical-error limits. From figure 1 the particles, for $W \leqslant 1$, settle on average with a velocity about 10 % greater than in still fluid. The increase is greatest at around $W = 1$ and decreases as W tends

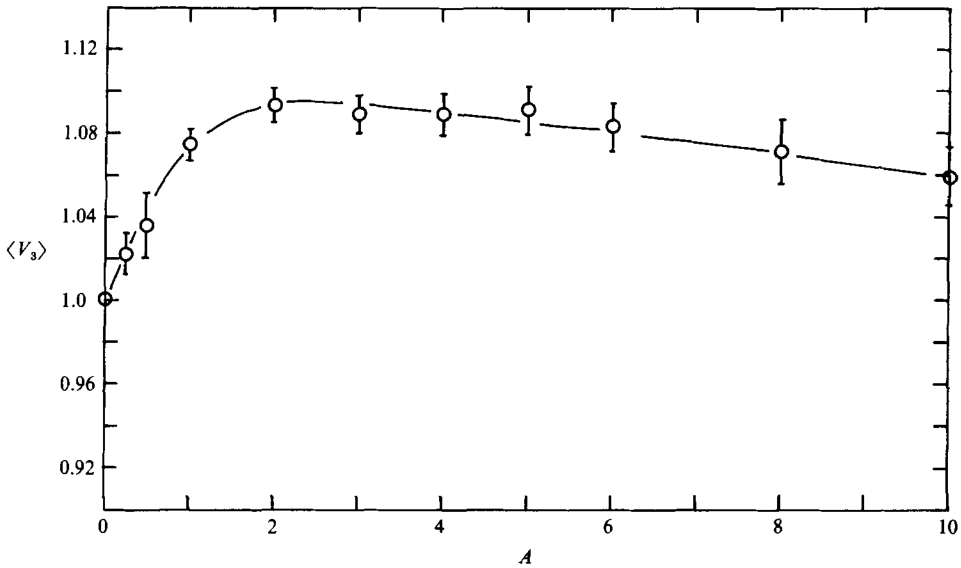

FIGURE 2. Simulation results for average settling velocity $\langle V_3 \rangle$ against inertia parameter A; still-fluid settling velocity $W = 1$ and $\omega_0 = 0$: ○, $\langle V_3 \rangle$. Statistical error bars are for one standard error.

to zero or as W increases beyond $W = 1$, being negligible for $W \geqslant 2$. Symmetry arguments imply that $\langle V_3 \rangle$ should vanish when W is zero.

Figure 2 shows the influence of the inertia parameter A on the average settling velocity for the fixed value of $W = 1$, again for the static flow field with infinite Eulerian timescale. T_E. The increase in settling velocity is seen to persist over a wide range of values of A, but falls off both in the limit of strong inertia, $A \rightarrow 0$, or of weak inertia, $A \rightarrow \infty$. Figure 3 shows the effect of varying the Eulerian integral time scale T_E, or equivalently by (3.11) of varying ω_0.

For large values of A the particle responds quickly to changes in the surrounding flow field and behaves much as if there were no inertia, in which case from §2.2 $\langle V_3 \rangle = W$. For small values of A, the particle inertia produces a lag in the response and reduces its magnitude so that the changing flow has less influence on the particle. An increase in the still-fluid settling velocity W or a reduction in the Eulerian correlation time T_E both tend to increase the rate at which the surrounding flow conditions change and particle inertia, for a fixed value of A, limits the response to either. Thus for example in the limit $\omega_0 \rightarrow \infty$, i.e. $T_E \rightarrow 0$, the value of $\langle V_3 \rangle$ should tend to W.

Further information is provided by the mean-square velocity fluctuations for both the particle velocity $\boldsymbol{V}(t)$ and the velocity of the particle relative to the fluid

$$\boldsymbol{w}(t) \equiv \boldsymbol{V}(t) - \boldsymbol{u}(\boldsymbol{Y}(t), t). \tag{3.13}$$

From (2.5) and (2.24) the long-term average value of $\boldsymbol{w}(t)$ is

$$\left.\begin{aligned} \langle \boldsymbol{w} \rangle_\infty &= \langle \boldsymbol{V}(t) \rangle_\infty - \langle \boldsymbol{u}(\boldsymbol{Y}(t), t) \rangle_\infty, \\ &= \boldsymbol{W}, \end{aligned}\right\} \tag{3.14}$$

where the subscript ∞ emphasizes the asymptotic value. Long after the particle

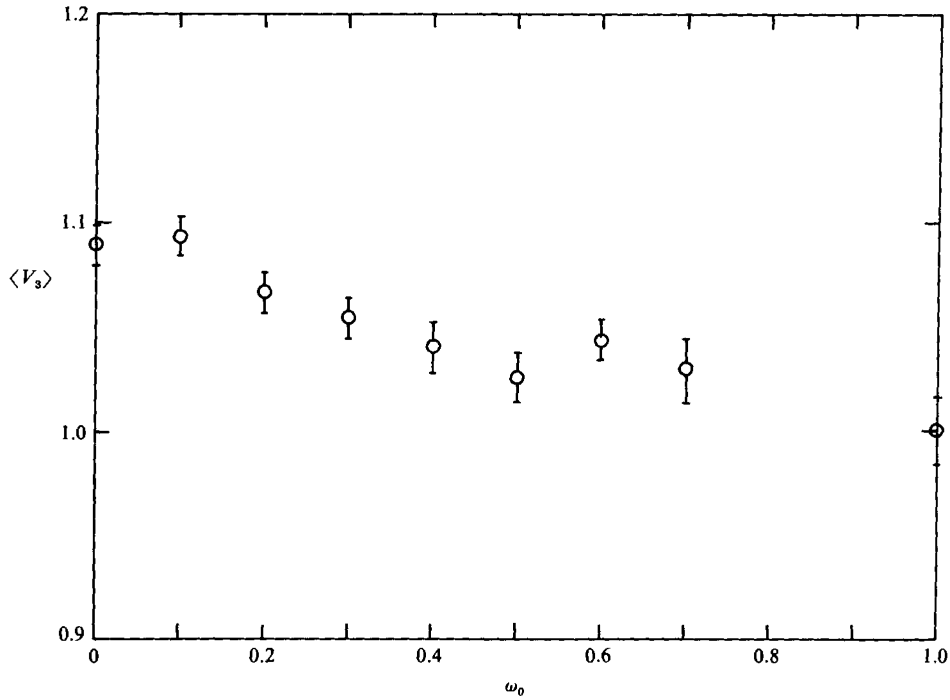

FIGURE 3. Variation in simulation results for $\langle V_3 \rangle$ with time-scale parameter ω_0; inertia parameter $A = 4$, still-fluid settling velocity $W = 1$: ○, $\langle V_3 \rangle$. The Eulerian integral time scale $T_E \propto 1/\omega_0$, see (3.11). Statistical error bars are shown.

release $\boldsymbol{w}(t)$, $\boldsymbol{V}(t)$, $\boldsymbol{u}(\boldsymbol{Y}(t),t)$ will all be statistically stationary and the fluctuations $\boldsymbol{w}'$ and $\boldsymbol{V}'$ may be defined as

$$\boldsymbol{w}'(t) = \boldsymbol{w}(t) - \boldsymbol{W}, \quad (3.15a)$$

$$\boldsymbol{V}'(t) = \boldsymbol{V}(t) - \langle \boldsymbol{V}(t) \rangle_\infty. \quad (3.15b)$$

Subtraction of the long-term average values from the equation of particle motion (2.4) gives

$$\frac{1}{A}\frac{\mathrm{d}\boldsymbol{V}'}{\mathrm{d}t} = -\boldsymbol{w}'(t). \quad (3.16)$$

Particle accelerations are finite, so we expect that the mean-square fluctuations in $\boldsymbol{w}'$ will decrease rapidly with increasing values of A.

Figure 4 shows the values of the mean-square particle-velocity fluctuations for $A = 1$ and varying values of W. The level of these fluctuations all decrease with increasing W for the qualitative reasons mentioned in the last but one paragraph, while the level of the fluctuations in the relative velocity $\boldsymbol{w}'$ increases. Figure 5 shows the effect of varying particle inertia for $\boldsymbol{W} = 1$. As the value of A increases the level of particle-velocity fluctuations increases markedly, tending to a value of 1.0. The arguments of §2.2 for motion in the absence of inertia may be extended to show that in the limit, $A \to \infty$,

$$\langle V_1'(t)^2 \rangle = \langle V_2'(t)^2 \rangle = \langle V_3'(t)^2 \rangle = \langle u_1^2(\boldsymbol{x},t) \rangle.$$

On the other hand the level of the relative velocity fluctuations decreases rapidly with increasing values of A. This is in accord with the comments above and (3.16); and often on the basis of small values of $\langle \boldsymbol{w}'(t)^2 \rangle$ inertia would be deemed to be a

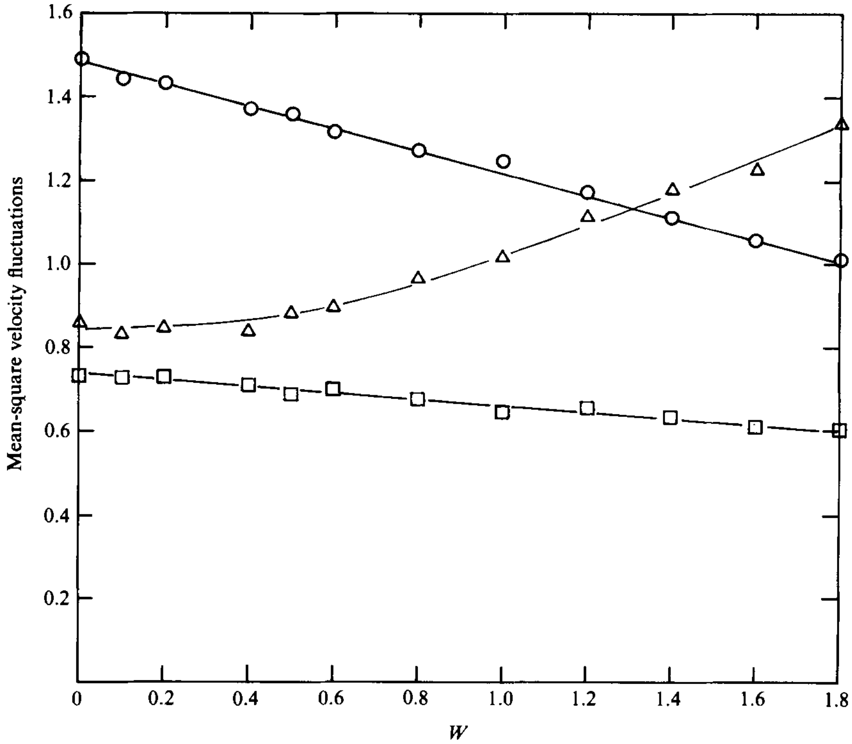

FIGURE 4. Simulation results for asymptotic mean-square particle-velocity fluctuations against still-fluid settling velocity W; $A = 1$ and $\omega_0 = 0$: ○, $\langle V_1'^2 + V_2'^2 \rangle$; □, $\langle V_3'^2 \rangle$; △, $\langle \boldsymbol{w}' \cdot \boldsymbol{w}' \rangle$.

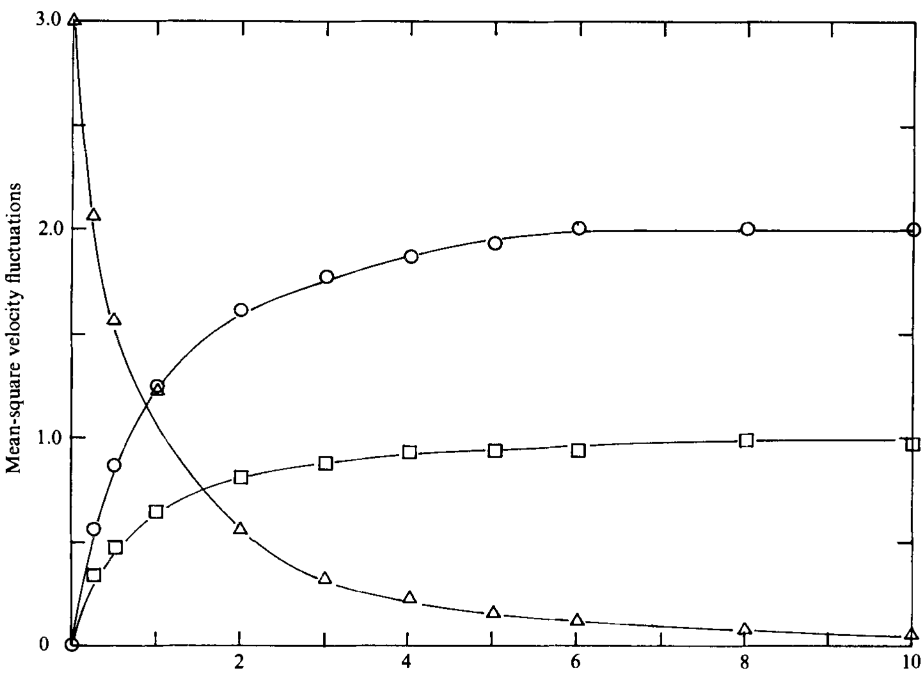

FIGURE 5. Simulation results for asymptotic mean-square particle-velocity fluctuations against inertia parameter A; $W = 1$ and $\omega_0 = 0$: ○, $\langle V_1'^2 + V_2'^2 \rangle$; □, $\langle V_3'^2 \rangle$; △, $\langle \boldsymbol{w}' \cdot \boldsymbol{w}' \rangle$.

negligible effect. However, while $\langle w'(t)^2 \rangle$ decreases by a factor of about 13 between $A = 1$ and 8 the value of the average settling velocity $\langle V_3 \rangle$ remains almost the same at about 8 or 10 % above the still-fluid value.

In a number of these simulations the flow field has been taken to be time-independent, with ω_0 set to zero and the Eulerian integral time scale T_E infinite. This helps partly to mitigate the shortcomings of the random-flow-field method. In genuine turbulence the Lagrangian motion of fluid elements becomes uncorrelated after a timescale of $O(L/u')$, while the influence of the small eddies decays over a time-scale comparable with the small-eddy turnover time. For the static random flow fields, where the eddies are essentially frozen in place, the Lagrangian motion becomes uncorrelated over a timescale of $O(L/u')$ as the fluid element wanders through the varying spatial structure of the flow field. The influence of the small eddies decays much more rapidly, being determined now by the time that a large eddy sweeps the fluid element through the small-scale eddy. If T_E is finite the Lagrangian correlation timescales in the random flow field are reduced and the motion of a fluid element becomes uncorrelated more quickly than if T_E were infinite. This accentuates the already rapid loss of correlation for the influence of the small eddies. In view of this the closest connection with turbulent flows probably comes with T_E large or infinite.

The simulation results provide conclusive evidence that the particle settling rates may be modified by the flow field, at least for the homogeneous random flow fields considered here. We may expect similar effects to occur in genuinely turbulent flows, but this remains to be verified and is presently being investigated. The problem remains, though, of establishing a mechanism responsible for this effect. To this end we now examine some asymptotic limits, first for a rapidly settling particle, $W \gg 1$, considered in the next section; and secondly for weak particle inertia, $A \gg 1$, considered in a later section. Our first aim is to establish on theoretical grounds that such a modification in settling rate should be found. Our second aim is to indicate the mechanism involved, for which at the end we use a combination of both asymptotic approximations.

4. Asymptotic analysis for rapid settling

4.1. *Expansion method*

In the limit of rapid settling, $W \gg 1$, the primary motion of the particle is to fall vertically along a straight-line trajectory. The influence of the flow field is then to produce perturbations to this basic motion. The equation (2.24) for the particle motion may be solved in terms of a perturbation expansion based on inverse powers of W,

$$\mathbf{Y}(t) = \mathbf{Y}^{(0)}(t) + \epsilon \mathbf{Y}^{(1)}(t) + \epsilon^2 \mathbf{Y}^{(2)}(t) + \epsilon^3 \mathbf{Y}^{(3)}(t) + \dots, \tag{4.1}$$

where formally $\epsilon = 1/W$ and terms are ordered according to their relative magnitude. The local fluid velocity is expanded in a Taylor series about $\mathbf{Y}^{(0)}(t)$ and the velocity derivatives are evaluated at $\mathbf{x} = \mathbf{Y}^{(0)}(t)$, at time t. The Taylor expansion allows the perturbation to be found explicitly and expressed eventually in terms of Eulerian data. The expansion is valid if $|\mathbf{Y}'|$, the departure of $\mathbf{Y}$ from $\mathbf{Y}^{(0)}$, is small compared to the lengthscale L of the flow field. As the particle settles rapidly with velocity $\mathbf{W}$ one may estimate in a qualitative sense an 'apparent frequency' at which the local flow field is changing as $W^{(s)}/L$, in dimensional form. So the effect on $\mathbf{Y}'$ of the fluid-velocity fluctuations of $O(u')$ is of order $O(u'L/W^{(s)})$, which is $O(L/W)$ and small compared to L. The original scalings are retained in the equation of motion, since these are the scales for the flow field $\boldsymbol{u}(\boldsymbol{x},t)$, and no attempt is made to rescale in terms of W. The parameter ϵ is used purely in a formal sense to identify terms of similar magnitude: to evaluate the final results ϵ is set equal to one. In the light of the above comments the fact that $Y^{(1)}$ is $O(1/W)$ will emerge naturally from the solutions.

Substitution of (4.1) into the equation of particle motion and the collection of the terms leads to a hierarchy of equations to be solved successively:

$$\frac{1}{A}\frac{\mathrm{d}^2 Y_i^{(0)}}{\mathrm{d}t^2}+\frac{\mathrm{d}Y_i^{(0)}}{\mathrm{d}t} = W_i, \tag{4.2}$$

$$\frac{1}{A}\frac{\mathrm{d}^2 Y_i^{(1)}}{\mathrm{d}t^2}+\frac{\mathrm{d}Y_i^{(1)}}{\mathrm{d}t} = u_i(\boldsymbol{Y}^{(0)}(t),t) \equiv u_i(t), \tag{4.3}$$

$$\frac{1}{A}\frac{\mathrm{d}^2 Y_i^{(2)}}{\mathrm{d}t^2}+\frac{\mathrm{d}Y_i^{(2)}}{\mathrm{d}t} = Y_j^{(1)}(t)\frac{\partial u_i(t)}{\partial x_j}, \tag{4.4}$$

$$\frac{1}{A}\frac{\mathrm{d}^2 Y_i^{(3)}}{\mathrm{d}t^2}+\frac{\mathrm{d}Y_i^{(3)}}{\mathrm{d}t} = Y_j^{(2)}(t)\frac{\partial u_i(t)}{\partial x_j}+\tfrac{1}{2}\, Y_j^{(1)}(t)\, Y_k^{(1)}(t)\frac{\partial^2 u_i(t)}{\partial x_j \partial x_k}, \tag{4.5}$$

$$\frac{1}{A}\frac{\mathrm{d}^2 Y_i^{(4)}}{\mathrm{d}t^2}+\frac{\mathrm{d}Y_i^{(4)}}{\mathrm{d}t} = Y_j^{(3)}(t)\frac{\partial u_i(t)}{\partial x_j}+ Y_j^{(1)}(t)\, Y_k^{(2)}(t)\frac{\partial^2 u_i(t)}{\partial x_j \partial x_k}$$
$$+\tfrac{1}{6} Y_j^{(1)}(t)\, Y_k^{(1)}(t)\, Y_m^{(1)}(t)\frac{\partial^3 u_i(t)}{\partial x_j \partial x_k \partial x_m}, \tag{4.6}$$

where we have introduced the notation $u_i(t)$ as in (4.3) to denote the velocity field evaluated at $\boldsymbol{Y}^{(0)}(t)$. These equations are solved subject to the initial conditions (3.12) as used in the simulations. The resulting solutions are given in Appendix A.

4.2. *Average settling velocity*

The long-term, asymptotic settling velocity $\langle \boldsymbol{V}(t)\rangle$ can be found by averaging (4.2)–(4.6) and summing the various contributions. Long after the particle release the velocity statistics are stationary and the average particle acceleration tends to zero. The average of (4.2) gives the long-term result

$$\left\langle\frac{\mathrm{d}Y_i^{(0)}}{\mathrm{d}t}\right\rangle = W_i, \tag{4.7}$$

so to leading order the average settling velocity is equal to the still-fluid settling velocity. Next an average of (4.3) gives

$$\left\langle\frac{\mathrm{d}Y_i^{(1)}}{\mathrm{d}t}\right\rangle = \langle u_i(\boldsymbol{x} = \boldsymbol{W}t,t)\rangle, \tag{4.8}$$

substituting for $\boldsymbol{Y}^{(0)}(t)$ from Appendix A. This is simply the Eulerian averaged mean fluid velocity, which is constant and for the purposes of the present discussion is set to zero. The average of (4.4), using the results of Appendix A, gives the long-term result

$$\left\langle\frac{\mathrm{d}Y_i^{(2)}}{\mathrm{d}t}\right\rangle = \int_0^t \mathrm{d}\tau\, \psi(t-\tau)\left\langle u_j(\tau)\frac{\partial u_i(t)}{\partial x_j}\right\rangle. \tag{4.9}$$

For homogeneous, incompressible turbulence the velocity-correlation term in the integrand vanishes and this contribution to the average settling velocity is zero.

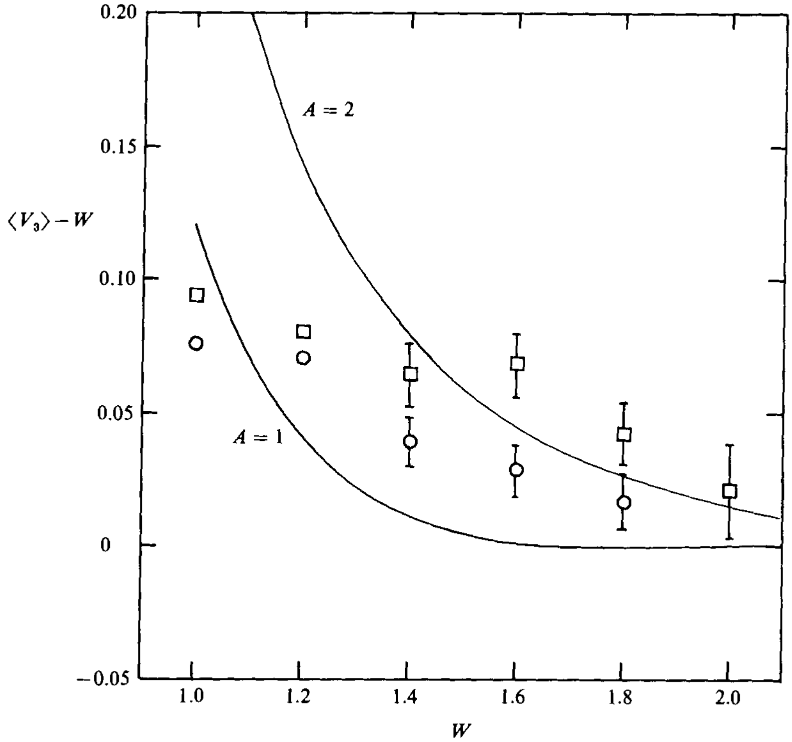

FIGURE 6. Comparison of the asymptotic estimates for the increase in average particle-settling velocity $\langle V_3\rangle - W$ with the simulation results as still-fluid settling velocity W varies; $\omega_0 = 0$: ○, simulation results for $A = 1$; □, simulation results for $A = 2$; ——, asymptotic estimates as labelled. Some statistical error bars are shown.

The first non-trivial contribution to the settling velocity comes at third order with the $Y^{(3)}$ term. The long-term average of (4.5) eventually gives the result

$$\left\langle \frac{\mathrm{d}Y_i^{(3)}}{\mathrm{d}t} \right\rangle = \int_0^t \mathrm{d}\tau \int_0^\tau \mathrm{d}\tau' \{\psi(t-\tau')\,\psi(t-\tau') - \psi(t-\tau)\,\psi(\tau-\tau')\} \times \left\langle \frac{\partial u_j}{\partial x_k}(\tau')\,\frac{\partial u_k}{\partial x_j}(\tau)\,u_i(t) \right\rangle, \quad (4.10)$$

using the results of Appendix A and the property of homogeneity. For a Gaussian velocity field, as in the simulations of the previous section, this three-point velocity correlation is zero since all odd-order correlations must vanish. In a general turbulent flow it will be non-zero and will contribute to the average particle-settling velocity. Its general form involves the fluid velocity at three distinct points evaluated at separate times and its specification requires knowledge of the three-point, space–time, triple velocity-correlation tensor. In general terms the effect of this contribution depends on the mechanisms of nonlinear energy transfer to small scales and the production of small-scale velocity fluctuations.

To obtain the first non-zero term that can be compared with the numerical simulations of §3, we must turn to the contribution from $Y^{(4)}$ and the long-term average of (4.6) for $\langle \mathrm{d}Y_i^{(4)}/\mathrm{d}t\rangle$. The specific evaluation of this term is quite complicated; the results are summarized in Appendix B. The contribution to the average settling velocity again is non-zero and involves four-point, fourth-order velocity correlations.

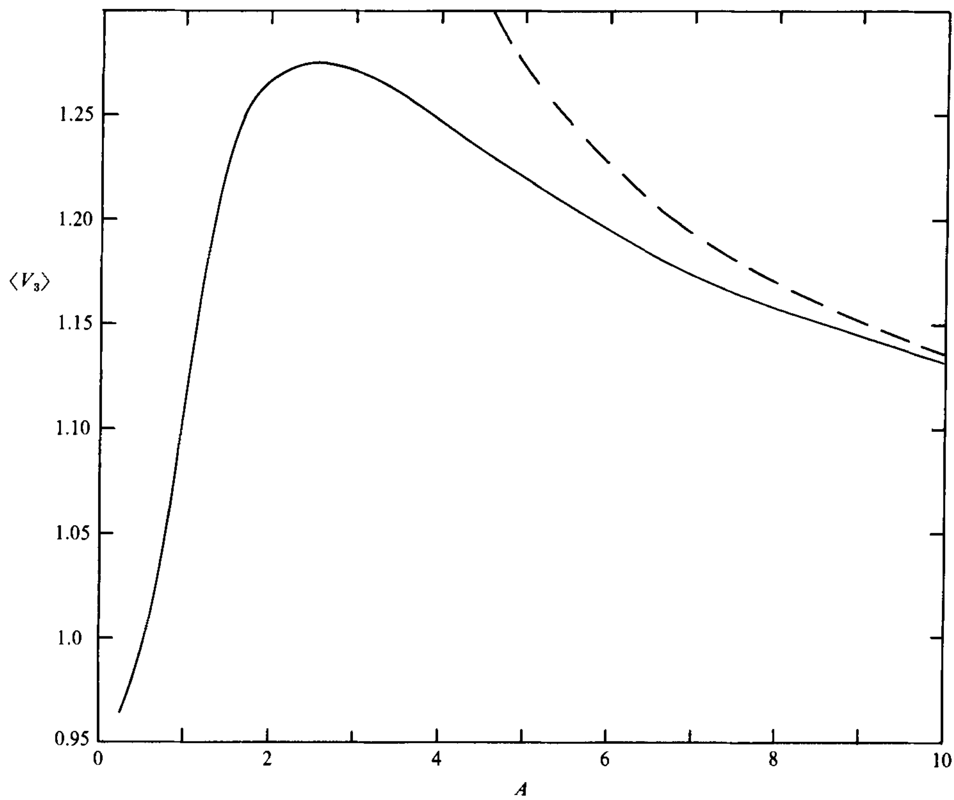

FIGURE 7. Asymptotic estimates for average settling velocity $\langle V_3 \rangle$ as inertia parameter A varies; $W = 1$ and $\omega_0 = 0$; ——, rapid settling; ----, rapid settling and weak particle inertia (see §6).

For the Gaussian velocity field these correlations may be expressed as combinations of the second-order velocity correlation. This simplification is used in Appendix B and leads to the final result given by (B 7). This has been evaluated for the correlation functions $f(r, \tau)$ and $g(r, \tau)$ as used in the simulations described in §3,

$$f(r,\tau) = \exp\left(-\tfrac{1}{2}k_0^2 r^2\right) \exp\left(-\tfrac{1}{2}\omega_0^2 \tau^2\right), \tag{4.11}$$

$$g(r,\tau) = \left(1-\tfrac{1}{2}k_0^2 r^2\right) f(r,\tau). \tag{4.12}$$

Figure 6 shows a comparison of these estimates of the average particle-settling velocity with the actual simulation results of the previous section. The estimates show the same basic trends although they do not agree closely with the simulations. The comparison improves for larger values of W, as may be expected for the asymptotic expansion, but for W larger than 2.0 the increase in settling velocity is quite small and the simulation results are subject to too much statistical error to make a close comparison. Figure 7 shows how the asymptotic estimate of average settling velocity varies with the inertia parameter A. The estimated increase in settling velocity is greatest around $A = 2$ to 5, again in the qualitative agreement with the simulations. Finally, figure 8 shows the influence of the correlation timescale T_E on these estimates. As may be expected the value of $\langle \mathrm{d} Y_3^{(4)}/\mathrm{d}t \rangle$ decreases for shorter correlation times, although there is a weak maximum around $\omega = 0.2$.

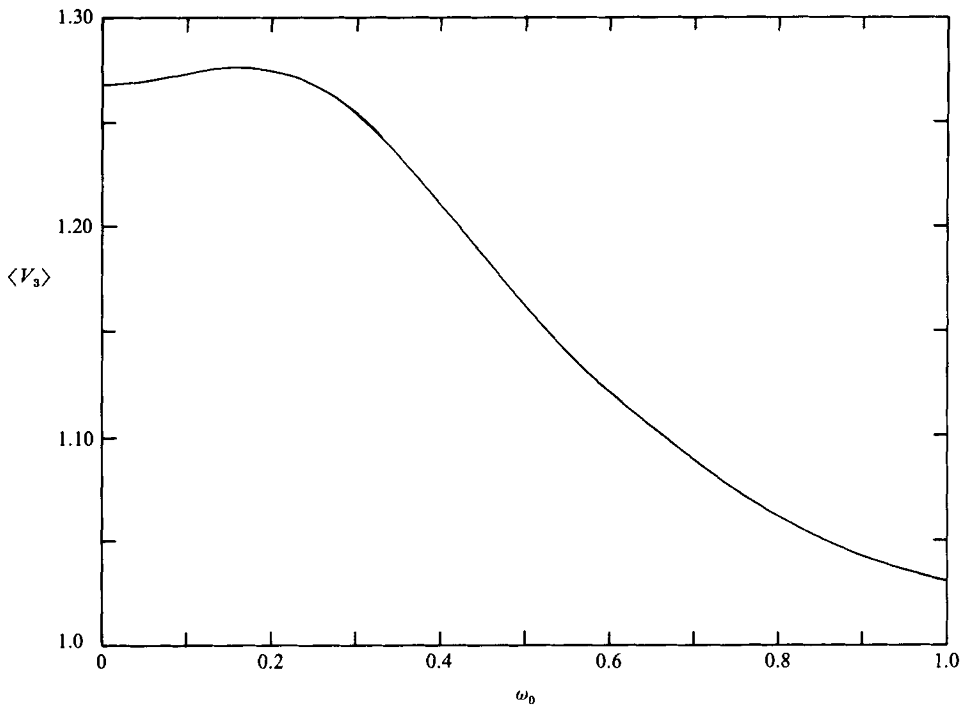

FIGURE 8. Asymptotic estimates for average settling velocity $\langle V \rangle_3$ as timescale parameter ω_0 varies; $W = 1$ and $A = 2$. The Eulerian integral timescale $T_E \propto 1/\omega_0$, see (3.11).

These asymptotic estimates exhibit the same basic trends as found in the simulations and indicate that the mechanism responsible for the increase in particle-settling velocity has been captured, at least approximately, by this expansion. The results for $\langle \mathrm{d}Y_i^{(3)}/\mathrm{d}t \rangle$ in (4.10) and $\langle \mathrm{d}Y_i^{(4)}/\mathrm{d}t \rangle$ in Appendix B in their present form do not provide an obvious intuitive explanation. To get a better understanding of these results we turn to a different asymptotic approximation based on the limit of small particle inertia, $A \gg 1$. In the next section this analysis is developed without other assumptions, and then finally is combined with the approximation for rapid settling to compare with the results here. The results of (4.10) and Appendix B could be expanded directly for $A \gg 1$ at this stage, but their interpretation would not be as clear.

5. Asymptotic analysis for small particle inertia

For many applications and certainly for most atmospheric contexts the particle inertia is small, so it is valuable to investigate the asymptotic approximation for $A \gg 1$. The most direct way to proceed is to formulate the equation of particle motion (2.24) as a nonlinear integral equation for $\boldsymbol{Y}(t)$ and then to expand this by integrating by parts. In integrated form the equation of particle motion is

$$\boldsymbol{Y}(t) = \boldsymbol{Y}(t=0) + \frac{1}{A}(\boldsymbol{V}(t=0) - \boldsymbol{W})[1 - \mathrm{e}^{-At}] + \boldsymbol{W}t + \int_0^t \tilde{\boldsymbol{u}}(t')[1 - \mathrm{e}^{-A(t-t')}]\,\mathrm{d}t', \quad (5.1)$$

where $$\tilde{\boldsymbol{u}}(t) \equiv \boldsymbol{u}(\boldsymbol{Y}(t),t). \tag{5.2}$$

Integration by parts then yields

$$\boldsymbol{Y}(t) = \boldsymbol{Y}(t=0)+\frac{1}{A}(\boldsymbol{V}(t=0)-\boldsymbol{W})+\boldsymbol{W}t+\int_0^t \tilde{\boldsymbol{u}}(t')\,\mathrm{d}t'-\frac{1}{A}\tilde{\boldsymbol{u}}(t)$$
$$+\mathrm{e}^{-At}\left[-\frac{1}{A}(\boldsymbol{V}(t=0)-\boldsymbol{W})+\frac{1}{A}\tilde{\boldsymbol{u}}(0)\right]+O\left(\frac{1}{A^2}\right). \tag{5.3}$$

At $t = 0$ there is a possibility for A $\gg 1$ of a rapid adjustment interval where the particle accelerates to match the surrounding flow conditions. This transient effect appears in (5.3) through the terms in $\exp(-At)$. It is also possible to specify an initial particle velocity so as to eliminate this rapid adjustment to the desired order of accuracy. Since we are interested in the long-term average properties of the particle motion, the choice of initial velocity conditions has no special significance. Thus we postulate

$$\boldsymbol{V}(t=0) = \boldsymbol{W}+\boldsymbol{u}(\boldsymbol{Y}(t=0),t=0), \tag{5.4}$$

so that

$$\boldsymbol{Y}(t) = \boldsymbol{Y}(t=0)+\frac{1}{A}\tilde{\boldsymbol{u}}(t=0)+\boldsymbol{W}t+\int_0^t \tilde{\boldsymbol{u}}(t')\,\mathrm{d}t'-\frac{1}{A}\tilde{\boldsymbol{u}}(t), \tag{5.5}$$

and the motion is on a timescale of $O(t)$ or slower.

A new differential equation for the particle motion is now obtained by differentiating (5.5):

$$\frac{\mathrm{d}\boldsymbol{Y}}{\mathrm{d}t} = \boldsymbol{W}+\tilde{\boldsymbol{u}}(t)-\frac{1}{A}\frac{\mathrm{d}\tilde{\boldsymbol{u}}}{\mathrm{d}t}. \tag{5.6}$$

The time derivatives $\mathrm{d}\tilde{\boldsymbol{u}}/\mathrm{d}t$ also depends on $\boldsymbol{Y}(t)$ and must be expanded in powers of $1/A$,

$$\frac{\mathrm{d}\tilde{\boldsymbol{u}}}{\mathrm{d}t} = \left.\left(\frac{\partial \boldsymbol{u}}{\partial t}+\frac{\mathrm{d}\boldsymbol{Y}}{\mathrm{d}t}\cdot\nabla\boldsymbol{u}\right)\right|_{\boldsymbol{Y}(t)}$$
$$= \left.\left(\frac{\partial \boldsymbol{u}}{\partial t}+(\boldsymbol{W}+\boldsymbol{u}(\boldsymbol{Y}(t),t))\cdot\nabla\boldsymbol{u}\right)\right|_{\boldsymbol{Y}(t)}+O\left(\frac{1}{A}\right).$$

The final form of the equation of motion is, correct to $O(1/A)$,

$$\frac{\mathrm{d}\boldsymbol{Y}}{\mathrm{d}t} = \boldsymbol{W}+\boldsymbol{u}(\boldsymbol{Y}(t),t)-\frac{1}{A}\left.\left(\frac{\partial \boldsymbol{u}}{\partial t}+(\boldsymbol{W}+\boldsymbol{u}(\boldsymbol{Y}(t),t))\cdot\nabla\boldsymbol{u}\right)\right|_{\boldsymbol{Y}(t)}. \tag{5.7}$$

This equation is first order and is simpler than the original second-order equation. The equation (5.7) is also accurate up to times t of $O(A)$ since the new equation is formulated as a new fully non-linear equation of motion that is to be solved numerically or otherwise. These results may be verified by a formal multiple-scale analysis and may be extended to higher-order terms.

The main advantage of (5.7) is that the velocity of the particle is completely specified by its instantaneous position. It is possible to define a particle velocity field $\boldsymbol{v}(\boldsymbol{x},t)$, as was done in §3, with

$$\frac{\mathrm{d}\boldsymbol{Y}}{\mathrm{d}t} = \boldsymbol{v}(\boldsymbol{x} = \boldsymbol{Y}(t),t), \tag{5.8}$$

$$\boldsymbol{v}(\boldsymbol{x},t) = \boldsymbol{u}(\boldsymbol{x},t)+\boldsymbol{W}+\frac{1}{A}\left(\frac{\partial \boldsymbol{u}}{\partial t}+\boldsymbol{u}\cdot\nabla\boldsymbol{u}+\boldsymbol{W}\cdot\nabla\boldsymbol{u}\right). \tag{5.9}$$

The distinction with the previous situation, where there was no particle inertia, is that for finite values of A the particle flow field is compressible and that

$$\nabla \cdot \boldsymbol{v} = -\frac{1}{A}\frac{\partial u_j}{\partial x_i}\frac{\partial u_i}{\partial x_j} \tag{5.10a}$$

$$= -\frac{1}{4A}\left\{\left(\frac{\partial u_i}{\partial x_j}+\frac{\partial u_j}{\partial x_i}\right)^2 - \left(\frac{\partial u_i}{\partial x_j}-\frac{\partial u_j}{\partial x_i}\right)^2\right\}. \tag{5.10b}$$

The divergence of the particle velocity field is positive in regions of high vorticity or low strain rate, and negative in regions where the strain rate dominates. Thus particles will tend to accumulate in regions of high strain rate or low vorticity. This also may be seen intuitively by considering a particle in a simple plane vortex flow with circular streamlines. If the particle were to follow the circular streamlines the effect of particle inertia would be to produce a drift outwards and the particle would spiral away from the vortex. Similarly in the pure straining flow near a stagnation point, the streamline curvature is reversed and inertia will cause the particle to drift towards the stagnation point.

One way to obtain the particle-averaged velocity statistics in homogeneous, stationary turbulence is to release a large number of particles, N_0, with an initially uniform distribution of the particles over some large volume Ω_0. The average particle velocity for example may be found by determining $\boldsymbol{V}(t)$ for each particle and then averaging over all the particles. This procedure may be repeated, if desired, to further obtain an ensemble average. The two averaging processes, though, should be equivalent because of the spatially ergodic nature of homogeneous, stationary turbulence provided that N_0 and Ω_0 are chosen to be large enough. Furthermore, the ensemble-averaged results should be independent of the initial particle position. The particle number density $n(\boldsymbol{x},t)$ is defined as the number of particles per unit volume† and is specified in the weak-inertia approximation by the 'conservation of particles' equation

$$\frac{\partial n}{\partial t} + \nabla \cdot (\boldsymbol{v}n) = 0, \tag{5.11}$$

where the initial number density $n(\boldsymbol{x},0)$ is specified and the possibility of particle interactions is excluded. In this manner then ensemble averaging and particle averaging may be combined to give, at some time t after the particle release,

$$\langle \boldsymbol{V}(t)\rangle = \frac{1}{N_0}\int \langle n(\boldsymbol{x},t)\,\boldsymbol{v}(\boldsymbol{x},t)\rangle\,\mathrm{d}^3\boldsymbol{x}, \tag{5.12}$$

where the integration volume is sufficiently large to contain all the particles and $n(\boldsymbol{x},t)\,\mathrm{d}^3\boldsymbol{x}$ represents the number of particles in the small volume $\mathrm{d}^3\boldsymbol{x}$ at the point $\boldsymbol{x}$ at time t.

A similar but more profitable approach is to take a fixed sample volume Ω contained in Ω_0 and to sum only over those particles contained in Ω. The corresponding estimate of the particle-averaged settling velocity is

$$[\boldsymbol{V}(t)]_\Omega = \frac{\int_\Omega n(\boldsymbol{x},t)\,\boldsymbol{v}(\boldsymbol{x},t)\,\mathrm{d}^3\boldsymbol{x}}{\int_\Omega n(\boldsymbol{x},t)\,\mathrm{d}^3\boldsymbol{x}}. \tag{5.13}$$

† In reality $n(\boldsymbol{x},t)/N_0$ is the probability-density function of particle position for a particle released at some random location in Ω_0. Each particle is introduced independently of the others with the same initial probability density.

The sample volume Ω should meet two requirements. First, the volume Ω, and hence Ω_0, should be large enough that the total number of particles in Ω remains close to the initial value of $n_0 \Omega$. Particles may enter or leave the sample volume only across the boundary surface and with a finite velocity, less than V_{max} say. The number of particles in Ω at some finite time t later on will be

$$\int_\Omega n(\boldsymbol{x},t)\,\mathrm{d}^3\boldsymbol{x} = \Omega n_0 + 0(\Omega^{\frac{2}{3}} V_{max} t n_0). \tag{5.14}$$

The relative error from neglecting the flux of particles in or out of Ω may be made arbitrarily small for large enough Ω. Secondly, the sample volume Ω should be a sufficiently small part of Ω_0 that any particle trajectory included in Ω at time t originated within Ω_0. Again this is possible because of the finite particle velocities, but the maximum possible size for Ω will shrink with time.

The equation of particle number density may be solved, at least formally, since from (5.11)

$$\frac{\mathrm{d}n}{\mathrm{d}t} = \frac{\partial n}{\partial t} + \boldsymbol{v}\cdot\nabla n = -n\nabla\cdot\boldsymbol{v}$$

and so

$$n(\boldsymbol{x},t) = n(\boldsymbol{Y}(0;\boldsymbol{x},t),0)\exp\left\{-\int_0^t \nabla\cdot\boldsymbol{v}[\boldsymbol{Y}(t';\boldsymbol{x},t)\,t']\,\mathrm{d}t'\right\}, \tag{5.15}$$

where the particle trajectory $\boldsymbol{Y}(t';\boldsymbol{x},t)$ is the solution of (5.8) satisfying the condition at time t that

$$\boldsymbol{Y}(t;\boldsymbol{x},t) = \boldsymbol{x}.$$

The second requirement on Ω ensures that if the point $\boldsymbol{x}$ lies within the sample volume at time t then the initial point of the trajectory $\boldsymbol{Y}(0;\boldsymbol{x},t)$ lies within Ω_0 and the initial number density is simply n_0. The results (5.14) and (5.15) when combined with (5.13) give the estimate of particle-averaged settling velocity based on the sample volume Ω as

$$[\boldsymbol{V}(t)]_\Omega = (\Omega n_0)^{-1}\int_\Omega \boldsymbol{v}(\boldsymbol{x},t)\,n_0\exp\left\{-\int_0^t \nabla\cdot\boldsymbol{v}[\boldsymbol{Y}(t';\boldsymbol{x},t),t']\,\mathrm{d}t'\right\}\mathrm{d}^3\boldsymbol{x}.$$

This may be combined with an ensemble average to obtain

$$\langle \boldsymbol{V}(t)\rangle = \frac{1}{\Omega}\int_\Omega \left\langle \boldsymbol{v}(\boldsymbol{x},t)\exp\left\{-\int_0^t \nabla\cdot\boldsymbol{v}[\boldsymbol{Y}(t';\boldsymbol{x},t),t']\,\mathrm{d}t'\right\}\right\rangle \mathrm{d}^3\boldsymbol{x}. \tag{5.16}$$

In a turbulent flow the effect of weak particle inertia should not lead to singular accumulations of particles and the number density $n(\boldsymbol{x},t)$ will deviate only slightly from its initially uniform value n_0. Thus the approximation of (5.15) to $O(1/A)$ is

$$n(\boldsymbol{x},t) = n_0\left\{1-\int_0^t \nabla\cdot\boldsymbol{v}[\boldsymbol{Y}(t';\boldsymbol{x},t),t']\,\mathrm{d}t'\right\}. \tag{5.17}$$

The long-term, average, particle-settling velocity obtained by substituting for $\boldsymbol{v}$ from (5.9) into (5.16) and using the approximation (5.17) is

$$\langle \boldsymbol{V}(t)\rangle = \boldsymbol{W} + \frac{1}{\Omega}\int_\Omega \langle \boldsymbol{u}(\boldsymbol{x},t)\rangle\,\mathrm{d}^3\boldsymbol{x} - \frac{1}{\Omega}\int_\Omega\int_0^t \langle \boldsymbol{u}(\boldsymbol{x},t)\nabla\cdot\boldsymbol{v}(\boldsymbol{Y}(t';\boldsymbol{x},t),t']\rangle\,\mathrm{d}t'\,\mathrm{d}^3\boldsymbol{x}, \tag{5.18}$$

for sufficiently large t. There is no need to include a term for $\langle \mathrm{d}\boldsymbol{u}/\mathrm{d}t\rangle$ since this is zero for large times.

The first volume integral in (5.18) reduces simply to $\boldsymbol{U}_0$, the value of the Eulerian mean fluid velocity $\langle \boldsymbol{u}(\boldsymbol{x},t)\rangle$ which is spatially uniform in homogeneous turbulence. If the particle velocity field were incompressible and $\nabla\cdot\boldsymbol{v}$ vanished then (5.18) would reduce to Lumley's result (Lumley 1962) quoted in §2.2. However, due to particle inertia $\nabla \cdot \boldsymbol{v}$ is non-zero and the second volume integral makes a net contribution to $\langle \boldsymbol{V}(t)\rangle$. It is this term that leads to changes in the particle-settling velocity. The correlation contained in the second integral of (5.18) is, from (5.10*a*),

$$\langle \boldsymbol{u}(\boldsymbol{x},t)\,\nabla\cdot\boldsymbol{v}[\boldsymbol{Y}(t';\boldsymbol{x},t),t']\rangle = -\frac{1}{A}\left\langle \boldsymbol{u}(\boldsymbol{x},t)\left(\frac{\partial u_k}{\partial x_m}\frac{\partial u_m}{\partial x_k}\right)\bigg|_{\boldsymbol{Y}(t';\boldsymbol{x},t)}\right\rangle. \tag{5.19}$$

This velocity correlation is evaluated along the particle trajectory $\boldsymbol{Y}(t';\boldsymbol{x},t)$, which itself fluctuates with the turbulence. However, the fixed reference point for the trajectory is the point $\boldsymbol{x}$ at time t, rather than the initial position of the particle, so that for homogeneous turbulence this ensembled-averaged correlation will be independent of the choice of $\boldsymbol{x}$. Again the volume integration may be eliminated with the final result that the long-term average particle velocity is

$$\langle \boldsymbol{V}(t)\rangle = \boldsymbol{W}+\boldsymbol{U}_0+\frac{1}{A}\int_0^t\left\langle \boldsymbol{u}(\boldsymbol{x},t)\left(\frac{\partial u_k}{\partial x_m}\frac{\partial u_m}{\partial x_k}\right)\bigg|_{\boldsymbol{Y}(t';\boldsymbol{x},t)}\right\rangle \mathrm{d}t'. \tag{5.20}$$

These preceding results illustrate the basic reason why the 1-point aerosol-particle velocity statistics differ from the corresponding Eulerian statistics. The departure of the average particle-settling velocity from the still-fluid value is determined by the accumulated bias of the particle trajectory towards regions of high strain rate or low vorticity and whether or not this bias is correlated with fluctuations in the local fluid velocity. Since it is the accumulated bias that is important, quite a large effect on the velocity statistics is possible even for large values of A. This was observed in the simulations where it was noted in §3 that $\langle V_3\rangle$ remained substantially the same while the fluctuations in the particle–fluid slip velocity w' decreased markedly with larger values of A. In certain situations, as in the cellular-flow-field computations of Maxey & Corrsin (1986), this bias may lead to singular accumulations of particles in narrowly confined regions. This is unlikely to occur in a turbulent flow though, because of the limited spatial and temporal correlations of the turbulence.

This bias of the trajectories is peculiar to motion in a non-uniform fluid flow and represents an important aspect of particle inertia. The more commonly noted effects of particle inertia – see for example Tchen (1947) – may equally be found in a uniform but unsteady flow field. In this situation particle inertia simply limits the response of the particle velocity to higher-frequency fluctuations in the flow field and introduces a phase lag in the response. An analysis which supposes that $\boldsymbol{u}(\boldsymbol{Y}(t),t)$ is somehow prescribed as a time series ignores the nonlinear coupling between the particle position and the local fluid velocity.

6. Combined limits of weak inertia and rapid settling

The result for the long-term average particle velocity (5.20) shows that the change in average settling velocity is determined by the integrated effect of the inertial bias towards regions of high strain rate or low vorticity, and the correlation of this with the turbulent-velocity fluctuations. While the integral in (5.20) may be expected to be non-zero in general, it remains an integral along particle trajectories and its evaluation requires computation of the individual trajectories, just as in the full simulations. Because of this path dependence the integral is non-zero even for a Gaussian random field. Some simpler estimates can be obtained for the asymptotic limit of rapid particle settling, where the basic particle trajectory is a straight vertical path with small deviation due to the turbulence. The technique is the same as developed in §4. The equation of particle motion, approximated for small particle inertia (5.7), is solved by successive approximation for $W \gg 1$ with the end condition that at time t the particle position is $\boldsymbol{x}$. The approximate particle trajectory corresponding to (4.1) is

$$\boldsymbol{Y}^{(0)}(t') = \boldsymbol{x} + \boldsymbol{W}(t'-t), \tag{6.1}$$

$$\boldsymbol{Y}^{(1)}(t') = -\int_{t'}^{t} \boldsymbol{u}(\boldsymbol{x} = \boldsymbol{Y}^{(0)}(t''), t'')\,\mathrm{d}t''. \tag{6.2}$$

Additional terms of order $1/A$ are neglected.

These two terms are enough to give the approximate results for weak particle inertia that correspond to $\langle \mathrm{d}\boldsymbol{Y}^{(3)}/\mathrm{d}t\rangle$ and $\langle \mathrm{d}\boldsymbol{Y}^{(4)}/\mathrm{d}t\rangle$, discussed in §4. There are no terms corresponding to $\langle \mathrm{d}\boldsymbol{Y}^{(1)}/\mathrm{d}t\rangle$ or $\langle \mathrm{d}\boldsymbol{Y}^{(2)}/\mathrm{d}t\rangle$ since the effect of a mean flow is already accounted for in (5.20) and the condition of homogeneous turbulence is already included in the derivation. The approximate change in settling velocity at lowest order is

$$\langle V_i^{(3)}\rangle = \frac{1}{A}\int_0^t \left\langle u_i(\boldsymbol{x},t)\left(\frac{\partial u_k}{\partial x_m}\frac{\partial u_m}{\partial x_k}\right)\bigg|_{\boldsymbol{Y}^{(0)}(t')}\right\rangle \mathrm{d}t', \tag{6.3}$$

which is the counterpart of (4.10). The next lowest contribution is

$$\langle V_i^{(4)}\rangle = -\frac{1}{A}\int_0^t \mathrm{d}t' \int_{t'}^{t} \mathrm{d}t'' \left\langle u_i(\boldsymbol{x},t)\,u_j(t'')\frac{\partial}{\partial x_j}\left(\frac{\partial u_k}{\partial x_m}\frac{\partial u_m}{\partial x_k}\right)\bigg|_{\boldsymbol{Y}^{(0)}(t')}\right\rangle, \tag{6.4}$$

which is the counterpart of the results in Appendix B. A Taylor-series expansion about the vertical path $\boldsymbol{Y}^{(0)}$ is used to evaluate the inertial bias term and $\boldsymbol{u}(t'')$ denotes the fluid velocity $\boldsymbol{u}$ evaluated at position $\boldsymbol{Y}^{(0)}(t'')$ at time t''.

These expressions for $\langle \boldsymbol{V}^{(3)}\rangle$ and $\langle \boldsymbol{V}^{(4)}\rangle$ are much simpler and more easily understood than the full forms given earlier. The result for $\langle \boldsymbol{V}^{(3)}\rangle$ depends on the two-point, Eulerian triple-velocity correlations. For general homogeneous turbulence these are non-zero, but will vanish for a Gaussian random field. The net effect of these correlations is also zero for isotropic turbulence because of the special symmetry properties. This may be seen by writing the inertial bias term as scalar S

$$S(\boldsymbol{x},t) = \left(\frac{\partial u_k}{\partial x_m}\frac{\partial u_m}{\partial x_k}\right)\bigg|_{(\boldsymbol{x},t)}, \tag{6.5}$$

and the triple correlation as

$$\left\langle u_i(\boldsymbol{x},t)\left(\frac{\partial u_k}{\partial x_m}\frac{\partial u_m}{\partial x_k}\right)\bigg|_{\boldsymbol{Y}^{(0)}(t')}\right\rangle = \langle u_i(\boldsymbol{x},t)\,S(\boldsymbol{x}',t')\rangle, \tag{6.6}$$

where $\boldsymbol{x}' = \boldsymbol{Y}^{(0)}(t')$ and the separation vector $(\boldsymbol{x}'-\boldsymbol{x})$ is $\boldsymbol{W}(t'-t)$. The overall correlation (6.6) is an isotropic vector field that must satisfy incompressibility. The combination of these conditions ensures that the correlation is zero (Batchelor 1953) and so $\langle \boldsymbol{V}^{(3)}\rangle$ is zero for isotropic turbulence. In view of this we may expect that the results found for the Gaussian random-flow simulations will be quite similar to those that would be observed in isotropic turbulence.

The expression for $\langle \boldsymbol{V}^{(4)}\rangle$, (6.4), depends on the three-point, Eulerian four-velocity correlations. These can be estimated for the Gaussian random flow using the procedures given in Appendix B and expressing the result in terms of second-order velocity correlations, to give finally the simplified result

$$\langle V_3^{(4)}\rangle = -\frac{2}{A}\int_0^t \mathrm{d}\tau \int_0^{\tau} \mathrm{d}\tau'\, H_3(\tau,\tau',\tau',t), \tag{6.7}$$

where the vector $\boldsymbol{H}$ is defined by (B 9) and (B 11) of Appendix B. A comparison of this result with the full expression given in §4 (see figure 7), shows that the approximation for weak particle inertia is accurate to within 10% for $A \geqslant 7$. This approximation for weak inertial effects is thus a useful approach for investigating the average statistics of particle motion.

These results for isotropic turbulence also show that it is the variations in the inertial bais term S as opposed to its absolute value that are important. The result (6.4) can be rewritten as

$$\langle V_i^{(4)} \rangle = \frac{1}{A} \int_0^t \mathrm{d}t' \, \langle u_i(\boldsymbol{x},t) \, \Delta S(t') \rangle, \tag{6.8}$$

Where the variation ΔS in inertial bias is the difference between S evaluated on the fluctuating trajectory and S evaluated along the vertical path $\boldsymbol{Y}^{(0)}$

$$\Delta S(t') = \boldsymbol{Y}^{(1)}(t') \cdot \nabla S(\boldsymbol{Y}^{(0)}(t'), t'). \tag{6.9}$$

As the particle settles vertically the turbulence produces fluctuations in the particle path which are weighted according to the corresponding fluctuations of ΔS, dependent on the local rate of strain or vorticity. The correlation of these fluctuations with $\boldsymbol{u}(\boldsymbol{x},t)$ determines the overall effect. The net result depends on the structure of the turbulent-velocity fluctuations, and these must be investigated in each context. Simple arguments about particles spending more time in updraughts than in downdraughts do not apply. The gravitational settling velocity $\boldsymbol{W}$ specifies a preferred direction, and as W increases limits the time over which the velocities in (6.4) remain correlated. For large values of W the correlations are limited by the spatial structure and only values of t', and hence t'', within $O(L/W)$ of t are relevant, where L is an appropriate integral lengthscale. Conversion of the integral (6.4) to an integral over spatial variables, using (6.1) and ignoring time variations in the flow field, shows that $\langle V^{(4)} \rangle$ decreases as $O(W^{-2})$ for large values of W.

7. Concluding remarks

The simulation results and asymptotic analyses show that there is no reason to expect aerosol particles to settle at the same rate in homogeneous turbulence with zero mean flow as in still fluid. Indeed, at least in the context of random flow fields with Gaussian statistics, the particles are shown to settle more rapidly over a wide range of conditions. The important mechanism for this is the effect of particle inertia and the bias this produces in the particle trajectories, for each realization of the turbulent flow, towards regions of high strain rate and/or low vorticity. The actual net effect of this bias on particle-settling velocities in a turbulent flow depends on the dynamics of the turbulence and the velocity correlations that naturally evolve.

The results presented here are preliminary in nature, and it remains to be seen what changes in settling velocity are observed in either experiments or direct simulations of homogeneous turbulence. In view of the results of the previous section for rapid particle settling and weak particle inertia, which show that triple correlations have no net effect, qualitatively similar results should be observed. Further, the techniques developed in §5 for analysing small inertia effects can equally be applied to other one-point particle statistics than the average settling velocity. They may be used for example to investigate mean-square fluctuations in particle velocity or in the relative velocity of the particle to the surrounding fluid.

I wish to thank Professor Stanley Corrsin for several helpful comments and profitable discussions during the course of this work. I am grateful to Andrew Smith for assisting with some of the computational simulations. This work was supported by a grant from the National Science Foundation (ATM-8310136).

Appendix A. Solutions for the successive approximations. $W \gg 1$.

The successive corrections to the particle motion in the case of rapid settling are given by the solutions of (4.2)–(4.5), subject to the initial conditions (3.12). The basic response $\boldsymbol{Y}^{(0)}(t)$ is, from (4.2) and (3.12),

$$\boldsymbol{Y}^{(0)}(t) = \boldsymbol{W}t. \tag{A1}$$

The solutions for $\boldsymbol{Y}^{(1)}(t)$, $\boldsymbol{Y}^{(2)}(t)$ and $\boldsymbol{Y}^{(3)}(t)$ are

$$\boldsymbol{Y}^{(1)}(t) = \int_0^t \psi(t-\tau)\, u_i(\tau)\, \mathrm{d}t, \tag{A2}$$

$$\boldsymbol{Y}^{(2)}(t) = \int_0^t \mathrm{d}\tau \int_0^\tau \mathrm{d}\tau'\, \psi(t-\tau)\, \psi(\tau-\tau')\, u_j(\tau') \frac{\partial u_i(\tau)}{\partial x_j}, \tag{A3}$$

$$\begin{aligned}\boldsymbol{Y}^{(3)}(t) = {} & \frac{1}{2}\int_0^t \mathrm{d}\tau \int_0^\tau \mathrm{d}\tau' \int_0^\tau \mathrm{d}\tau''\, \psi(t-\tau)\, \psi(\tau-\tau')\, \psi(\tau-\tau'')\, u_j(\tau')\, u_k(\tau'') \frac{\partial^2 u_i(\tau)}{\partial x_j\, \partial x_k} \\ & + \int_0^t \mathrm{d}\tau \int_0^\tau \mathrm{d}\tau' \int_0^{\tau'} \mathrm{d}\tau''\, \psi(t-\tau)\, \psi(\tau-\tau')\, \psi(\tau'-\tau'')\, u_j(\tau'') \frac{\partial u_k(\tau')}{\partial x_j} \frac{\partial u_i(\tau)}{\partial x_k}.\end{aligned} \tag{A4}$$

The integrating factor $\psi(s)$ is

$$\psi(s) = 1-\exp(-As). \tag{A5}$$

Appendix B. Evaluation of $\langle \mathrm{d}Y_i^{(4)}/\mathrm{d}t\rangle$ for the Gaussian velocity field

The component terms from the average of (4.6) for $\langle \mathrm{d}Y_i^{(4)}/\mathrm{d}t\rangle$ may be divided into three groups. First,

$$\begin{aligned}\left\langle Y_j^{(3)}(t) \frac{\partial u_i(t)}{\partial x_j}\right\rangle = {} & \frac{1}{2}\int_0^t \mathrm{d}\tau\, \psi(t-\tau) \int_0^\tau \mathrm{d}\tau' \int_0^\tau \mathrm{d}\tau'' \Big\{\psi(\tau-\tau')\, \psi(\tau-\tau'') \\ & \times \left\langle u_k(\tau')\, u_m(\tau'') \frac{\partial^2 u_j(\tau)}{\partial x_k \partial x_m} \frac{\partial u_i(t)}{\partial x_j}\right\rangle\Big\} + \int_0^t \mathrm{d}\tau\, \psi(t-\tau) \int_0^\tau \mathrm{d}\tau' \int_0^{\tau'} \mathrm{d}\tau'' \\ & \times \left\{\psi(\tau-\tau')\, \psi(\tau'-\tau'') \left\langle u_k(\tau'') \frac{\partial u_m(\tau')}{\partial x_k} \frac{\partial u_j(\tau)}{\partial x_m} \frac{\partial u_i(t)}{\partial x_j}\right\rangle\right\}.\end{aligned} \tag{B1}$$

This expression depends on the fourth-order velocity correlation tensor, which in turn may be written in terms of the second-order velocity correlations on the assumption that the velocity statistics are jointly Gaussian. This assumption implies that

$$\begin{aligned}\langle u_k(\boldsymbol{x},t)\, u_m(\boldsymbol{x}',t')\, u_j(\boldsymbol{x}'',t'')\, u_i(\boldsymbol{x}''',t''')\rangle = {} & \langle u_k(\boldsymbol{x},t)\, u_m(\boldsymbol{x}',t')\rangle \\ & \times \langle u_j(\boldsymbol{x}'',t'')\, u_i(\boldsymbol{x}''',t''')\rangle + \langle u_k(\boldsymbol{x},t)\, u_j(\boldsymbol{x}'',t'')\rangle \langle u_m(\boldsymbol{x}',t')\, u_i(\boldsymbol{x}''',t''')\rangle \\ & + \langle u_k(\boldsymbol{x},t)\, u_i(\boldsymbol{x}''',t''')\rangle \langle u_m(\boldsymbol{x}',t)\, u_j(\boldsymbol{x}'',t'')\rangle.\end{aligned} \tag{B2}$$

When (B2) is used in (B1) a number of the terms cancel because of the homogeneity or the incompressibility of the flow. In fact, all the terms in the first integral of (B1) cancel in this fashion. From the second integral only one term remains and so finally

$$\left\langle Y_j^{(3)} \frac{\partial u_i(t)}{\partial x_j} \right\rangle = \int_0^t \mathrm{d}\tau\, \psi(t-\tau) \int_0^\tau \mathrm{d}\tau' \int_0^{\tau'} \mathrm{d}\tau'' \Big\{ \psi(\tau-\tau')\, \psi(\tau'-\tau'') \times \left\langle u_k(\tau'') \frac{\partial u_j(\tau)}{\partial x_m} \right\rangle \left\langle \frac{\partial u_m(\tau')}{\partial x_k} \frac{\partial u_i(t)}{\partial x_j} \right\rangle \Big\}. \quad \text{(B3)}$$

The second group of terms is

$$\left\langle Y_j^{(1)}(t)\, Y_k^{(2)}(t) \frac{\partial^2 u_i(t)}{\partial x_j \partial x_k} \right\rangle = \int_0^t \mathrm{d}\tau\, \psi(t-\tau) \int_0^t \mathrm{d}\tau' \int_0^{\tau'} \mathrm{d}\tau'' \Big\{ \psi(t-\tau')\, \psi(\tau'-\tau'') \times \left\langle u_j(\tau)\, u_m(\tau'') \frac{\partial u_k(\tau')}{\partial x_m} \frac{\partial^2 u_i(t)}{\partial x_j \partial x_k} \right\rangle \Big\}. \quad \text{(B4)}$$

This simplifies for the same reasons and only one term makes a final contribution, so

$$\left\langle Y_j^{(1)}(t)\, Y_k^{(2)}(t) \frac{\partial^2 u_i(t)}{\partial x_j \partial x_k} \right\rangle = \int_0^t \mathrm{d}\tau\, \psi(t-\tau) \int_0^t \mathrm{d}\tau' \int_0^{\tau'} \mathrm{d}\tau'' \Big\{ \psi(t-\tau')\, \psi(\tau'-\tau'') \times \left\langle u_j(\tau) \frac{\partial u_k(\tau')}{\partial x_m} \right\rangle \left\langle u_m(\tau'') \frac{\partial^2 u_i(t)}{\partial x_i \partial x_k} \right\rangle \Big\}. \quad \text{(B5)}$$

In the same manner the third group may be simplified and in fact

$$\frac{1}{6} \left\langle Y_j^{(1)}(t)\, Y_k^{(1)}(t)\, Y_m^{(1)}(t) \frac{\partial^3 u_i(t)}{\partial x_j \partial x_k \partial x_m} \right\rangle = \int_0^t \mathrm{d}\tau \int_0^t \mathrm{d}\tau' \int_0^t \mathrm{d}\tau'' \Big\{ \psi(t-\tau) \times \psi(t-\tau')\, \psi(t-\tau'') \left\langle u_j(\tau)\, u_k(\tau')\, u_m(\tau'') \frac{\partial^3 u_i(t)}{\partial x_j \partial x_k \partial x_m} \right\rangle \Big\} = 0. \quad \text{(B6)}$$

These component terms (B3) and (B5) combined give the value of $\langle \mathrm{d} Y_i^{(4)}/\mathrm{d}t \rangle$ as

$$\left\langle \frac{\mathrm{d} Y_i^{(4)}}{\mathrm{d}t} \right\rangle = \int_0^t \mathrm{d}\tau\, \psi(t-\tau) \Big\{ \int_0^t \mathrm{d}\tau' \int_0^{\tau'} \mathrm{d}\tau''\, \psi(t-\tau')\, \psi(\tau'-\tau'')\, H_i(\tau,\tau',\tau'',t) + \int_0^\tau \mathrm{d}\tau' \int_0^{\tau'} \mathrm{d}\tau''\, \psi(\tau-\tau')\, \psi(\tau'-\tau'')\, H_i(\tau,\tau'',\tau',t) \Big\}, \quad \text{(B7)}$$

where the property of homogeneity is used to rearrange the derivatives in (B3) and H_i is defined to be

$$H_i(\tau,\tau',\tau'',t) \equiv \left\langle u_j(\tau) \frac{\partial u_k(\tau')}{\partial x_m} \right\rangle \left\langle u_m(\tau'') \frac{\partial^2 u_i(t)}{\partial x_j \partial x_k} \right\rangle. \quad \text{(B8)}$$

This correlation may be simplified further in the context of isotropic turbulence, using the two-point correlation tensor of (2.14), (2.15),

$$H_i(\tau,\tau',\tau'',t) = \frac{\partial}{\partial s_m} R_{jk}(\boldsymbol{s},\tau'-\tau) \frac{\partial^2}{\partial r_j \partial r_k} R_{mi}(\boldsymbol{r},t-\tau''). \quad \text{(B9)}$$

where the correlations are evaluated for

$$\boldsymbol{s} = (\tau'-\tau)\, \boldsymbol{W}, \quad \boldsymbol{r} = (t-\tau'')\, \boldsymbol{W}. \quad \text{(B10)}$$

The final desired result is for $H_3(\tau,\tau',\tau'',t)$ with $\boldsymbol{W} = (0,0,W)$, and in view of (B10) this means that

$$\boldsymbol{s} = (0,0,s \operatorname{sgn}(\tau'-\tau))$$

and

$$\boldsymbol{r} = (0,0,r \operatorname{sgn}(t-\tau'')).$$

Some manipulation then leads to the final result for H_3

$$H_3(\tau,\tau',\tau'',t) = \mathrm{sgn}\,(\tau'-\tau)\left\{2\frac{\partial^2}{\partial r^2}f(r,t-\tau'')\frac{\partial}{\partial s}f(s,\tau'-\tau) + \frac{4}{r}\frac{\partial}{\partial r}f(r,t-\tau'')\frac{\partial}{\partial s}g(s,\tau'-\tau)\right\}. \quad \text{(B 11)}$$

REFERENCES

BATCHELOR, G. K. 1953 *The Theory of Homogeneous Turbulence*. Cambridge University Press.

CLIFT, R., GRACE, J. R. & WEBER, M. E. 1978 *Bubbles, Drops and Particles*. Academic.

CSANADY, G. T. 1963 Turbulent diffusion of heavy particles in the atmosphere. *J. Atmos. Sci.* **20**, 201–208.

KRAICHNAN, R. H. 1970 Diffusion by a random velocity field. *Phys. Fluids* **13**, 22–31.

LUMLEY, J. L. 1962 The mathematical nature of the problem of relating Lagrangian and Eulerian statistical functions in turbulence. In *Mécanique de la Turbulence* (ed. A. Favre), pp. 17–26. Paris, CRNS.

MAXEY, M. R. & CORRSIN, S. 1986 Gravitational settling of aerosol particles in randomly oriented cellular flow fields. *J. Atmos. Sci.*, **43**, 1112–1134.

MAXEY, M. R. & RILEY, J. J. 1983 Equation of motion for a small rigid sphere in a nonuniform flow. *Phys. Fluids* **26**, 883–889.

MEEK, C. C. & JONES, B. G. 1973 Studies of the behaviour of heavy particles in a turbulent fluid flow. *J. Atmos. Sci.* **30**, 239–244.

NIR, A. & PISMEN, L. M. 1979 The effect of steady drift on the dispersion of a particle in turbulent fluid. *J. Fluid Mech.* **94**, 369–381.

PRUPPACHER, H. R. & KLETT, J. D. 1978 *Microphysics of Clouds and Precipitation*. Reidel.

REEKS, M. W. 1977 On the dispersion of small particles suspended in an isotropic turbulent fluid. *J. Fluid Mech.* **83**, 529–546.

REEKS, M. W. 1980 Eulerian direct interaction applied to the statistical motion of particles in a turbulent fluid. *J. Fluid Mech.* **97**, 569–590.

RICE, J. R. 1983 *Numerical Methods, Software and Analysis: I.M.S.L. Reference Edition*. McGraw-Hill.

RILEY, J. J. 1971 Computer simulations of turbulent dispersion. Ph.D. thesis., The Johns Hopkins University, Baltimore.

RILEY, J. J. & PATTERSON, G. S. 1974 Diffusion experiments with numerically integrated isotropic turbulence. *Phys. Fluids* **17**, 292–297.

SNYDER, W. H. & LUMLEY, J. L. 1971 Some measurements of particle velocity autocorrelation functions in a turbulent flow. *J. Fluid Mech.* **48**, 41–71.

TCHEN, C. M. 1947 Mean value and correlation problems connected with the motion of small particles suspended in a turbulent fluid. Ph.D. thesis, Delft; The Hague, Martinus Nijhoff.

TENNEKES, H. & LUMLEY, J. L. 1972 *A First Course in Turbulence*. M.I.T. Press.

WELLS, M. R. & STOCK, D. E. 1983 The effects of crossing trajectories on the dispersion of particles in a turbulent flow. *J. Fluid Mech.* **136**, 31–62.

YUDINE, M. I. 1959 Physical considerations on heavy particle diffusion. *Adv. Geophys.* **6**, 185–191.